ATOM TRANSFER RADICAL POLYMERIZATION FROM MULTIFUNCTIONAL SUBSTRATES

Anna Carlmark

Department of Polymer Technology
Royal Institute of Technology
Stockholm 2002

AKADEMISK AVHANDLING

Som med tillstånd av Kungliga Tekniska Högskolan i Stockholm framlägges till offentlig granskning för avläggande av teknisk licentiatexamen tisdagen den 11 juni 2002, kl 10.00 i sal K1, Teknikringen 56, KTH, Stockholm.

ABSTRACT

Atom transfer radical polymerization (ATRP) has proven to be a powerful technique to obtain polymers with narrow polydispersities and controlled molecular weight. It also offers control over chain-ends. The technique is the most studied and utilized of the controlled/"living" radical polymerization techniques since a large number of monomers can be polymerized under simple conditions. ATRP can be used to obtain polymer grafts from multifunctional substrates. The substrates can be either soluble (*i. e*. based on dendritic molecules) or insoluble (such as gold or silicon surfaces). The large number of growing chains from the multifunctional substrates increases the probability of inter-and intramolecular reactions. In order to control these kinds of polymerizing systems, and suppress side-reactions such as termination, the concentration of propagating radicals must be kept low. To elaborate such a system a soluble multifunctional substrate, based on 3-ethyl-3-(hydroxymethyl)oxetane, was synthesized. It was used as a macroinitiator for the atom transfer radical polymerisation of methyl acrylate (MA) mediated by Cu(I)Br and tris(2-(dimethylamino)ethyl)amine (Me_6-TREN) in ethyl acetate at room temperature. This yielded a co-polymer with a dendritic-linear architecture. Since most solid substrates are sensitive to the temperatures at which most ATRP polymerisations are performed, lowering the polymerization temperatures are preferred. ATRP at ambient temperature is always more desirable since it also suppresses the formation of thermally formed polymer. The macroinitiator contained approximately 25 initiating sites, which well mimicked the conditions on a solid substrate. The polymers had low polydispersity and conversions as high as 65% were reached without loss of control. The solid substrate of choice was cellulose fibers that prior to this study not had been grafted through ATRP. As cellulose fibers a filter paper, Whatman 1, was used due to its high cellulose content. The hydroxyl groups on the surface was first reacted with 2-bromoisobutyryl bromide followed by grafting of MA. Essentially the same reaction conditions were used that had been elaborated from the soluble substrate. The grafting yielded fibers that were very hydrophobic (contact angles>100°). By altering the sacrificial initiator-to-monomer ratio the amount of polymer that was attached to the surface could be tailor. PMA with degrees of polymerization (DP's) of 100, 200 and 300 were aimed. In order to control that the polymerizations from the surface was indeed "living" a second layer of a hydrophilic monomer, 2-hydroxymethyl methacrylate (HEMA), was grafted onto the surface. This dramatically changed the hydrophobic behavior of the fibers.

LIST OF PAPERS

This thesis is a summary of the following papers:

I "Atom Transfer Radical Polymerization of Methyl Acrylate from a Multifunctional Initiator at Ambient Temperature", A. Carlmark, R. Vestberg, E. Malmström, *Polymer,* **2002**, *in press*

II "Atom Transfer Radical Polymerization from Cellulose Fibers at Ambient Temperature", A. Carlmark, E. Malmström, *Journal of the American Chemical Society,* **2002**, *124(6)*, 900-901

The thesis also contains unpublished results.

TABLE OF CONTENTS

INTRODUCTION

FREE RADICAL POLYMERIZATION

Free radical polymerization is one of the most widely used industrial polymerization methods. The advantages with this technique are its low requirements on reactant purity and that a wide variety of polymers can be polymerized and co-polymerized under simple conditions. However, this method offers no control over the molecular weights and polydispersities of the resulting polymer. The high concentration of reactive free radicals causes side reactions, such as termination and chain transfer, to take place to a great extent. More controlled polymerization techniques are needed for polymers with higher demands on a well-defined structure. Reactions where no termination takes place and the polymerization proceeds in a control manner and continues until all the monomers are consumed, are termed living. Living cationic, anionic and group-transfer polymerizations are examples of such techniques. However, these reactions are synthetically demanding, as they require high purity of the reactants as well as the absence of both oxygen and water, which limits their industrial use. More controlled radical polymerization techniques have therefore been developed such as atom transfer radical polymerization (ATRP), reversible addition fragmentation chain transfer (RAFT) and the nitroxide mediated free radical process (NMP).

ATOM TRANSFER RADICAL POLYMERIZATION (ATRP)

One of the most widely studied controlled radical polymerization techniques is atom transfer radical polymerization (ATRP). ATRP has been thoroughly investigated since it was developed independently by Matyjaszewski and Wang[1-2] and Sawamoto *et al.*[3] in 1995. It was developed from redox catalyzed telomerization reactions[4] as well as from atom transfer radical addition (ATRA),[5] Scheme 1. ATRA is a modification of the Kharasch addition reaction, in which a transition metal catalyst acts as a carrier of the halogen atom in a reversible redox process.[6-7] ATRP has proven to be a powerful tool in the synthesis of polymers with narrow polydispersities and controlled molecular

weights.[8] However, termination reactions are only minimized in ATRP and the reaction is therefore termed controlled/"living" polymerization.[2,9]

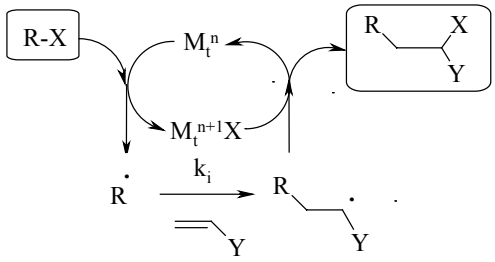

Scheme 1. Atom Transfer Radical Addition (ATRA).

Components in ATRP

All ATRP systems are composed of monomer, initiator and catalyst (transition metal and a suitable ligand).

Monomers

Various vinyl monomers have successfully been polymerized with ATRP. Most investigated are polymerization of styrenes,[2,10-13] acrylates[1-2,14-18] and methacrylates,[13,17,19-26] but other monomers such as acrylonitrile,[27-28] (meth)acrylamide,[29-31] and other compounds containing substituents that can stabilize a propagating radical have proven successful as well. These monomers have been polymerized under different ATRP conditions, and which conditions that should be used are specific for each monomer. Some examples of monomers that have been polymerized with ATRP are shown in Figure 1.

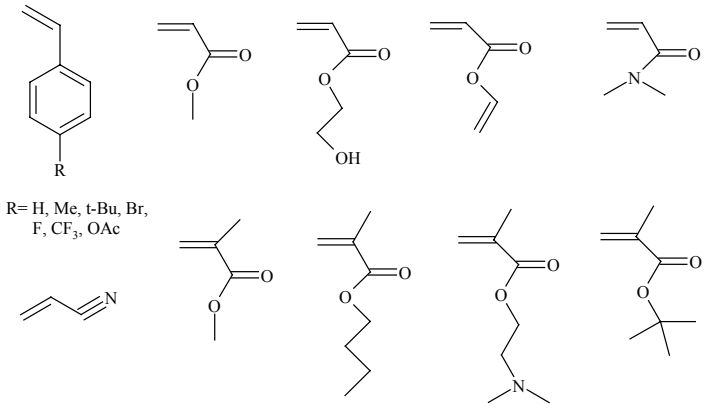

Figure 1. Examples of monomers that can be polymerized with ATRP.

Initiators

The initiator generates the growing chains, thus, the initiator concentration determines the molecular weight of the resulting polymer. The theoretical degree of polymerization (DP) can be calculated according to equation 1.[32]

$$DP = \frac{[M]_0}{[I]_0} * conversion \quad (1)$$

In ATRP the initiator is typically an alkyl halide (RX). It is important that the initiation rate is higher than the propagating rate, in order to get all the chains growing at the same time. If initiation is incomplete at the beginning of the reaction this will lead to higher molecular weights than the targeted ones and higher polydispersities.[33] Another important factor is that the initiator shows little or no tendency to undergo side reactions. It has been shown that tertiary alkyl halides are better initiators than secondary ones, which are better than primary ones. Other variables that are important to take into account when choosing an initiator are steric, polar and redox properties.[34] One easy rule to follow is that the R-group in the alkyl halide should be similar in structure to that of the monomer. For example, (1-bromoethyl)benzene is usually used when polymerizing styrene.[2] Compounds such as ethyl 2-bromoisobutyrate and ethyl 2-bromopropionate are used for meth(acrylates)[34] and 2-bromopropionitrile can be used for acrylonitiles.[27-28] However, other initiators work well for different monomers. Some examples of initiators are shown in Figure 2. The alkyl is usually bromide or chlorine. ATRP of acrylates[35] and styrene[11-12] with iodine-based initiators has been reported. Fluorine does not work in ATRP due to the strong H-F bond, which cannot undergo homolytic cleavage.

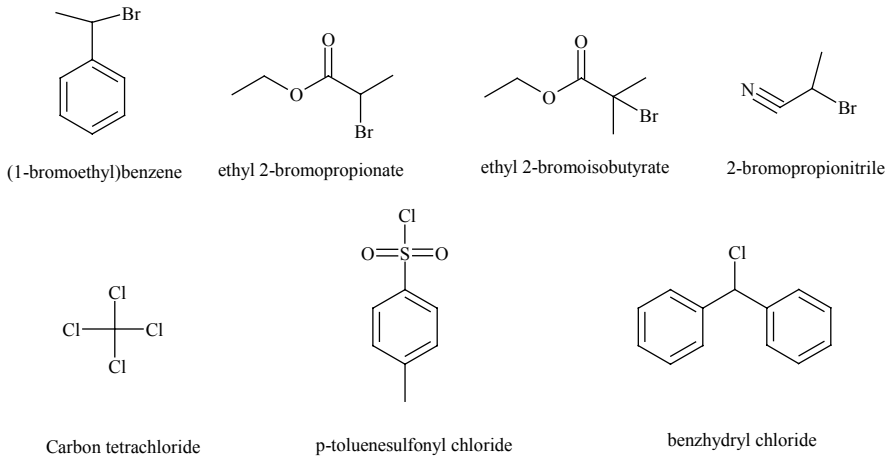

Figure 2. Examples of initiators for ATRP.

Transition metals

Several transition metals have been used in ATRP. Copper is by far the most widely used metal due to its versatility in ATRP and relatively low cost. However, other metals such as iron,[13,25,36] ruthenium,[3,37-40] nickel,[23,41-42] molybdenum[43-44] rhenium,[35] rhodium,[45] and palladium[46] have also proven successful for various monomers. The requirements on the metal are that it should have an accessible one-electron redox couple, it should have reasonable affinity towards a halogen and the coordination sphere around the metal should be able to increase by one upon oxidation in order to selectively accommodate a new ligand. Also, the metal should have a low affinity for other atoms such as hydrogen atoms and alkyl radicals.[34]

Ligands

A large variety of ligands have been used in conjunction with the different transition metals. The ligands are an important part of the ATRP system and its role is three-fold. First, the ligand solubilize the metal in the organic reaction media. Second, they control selectivity by steric and electronic effects. Finally, by their electronic effects they also affect the redox chemistry of the final metal complex. Copper is usually ligated with nitrogen-based ligands. Figure 3 shows some examples of bidentate (4,4'-di-5-nonyl-2,2'-bipyridine, dNbpy and 2,2'-bipyridine, Bipy)[1], tridentate (pentamethyldiethylenetriamine, PMDETA)[47] and tetradentate (tris(2-(dimethylamino)ethyl)amine, Me_6-TREN)[48] ligands that have successfully been used in copper-based ATRP. The bidentate ligands are believed to ligate with two molecules (Figure 4) while the others with only one.

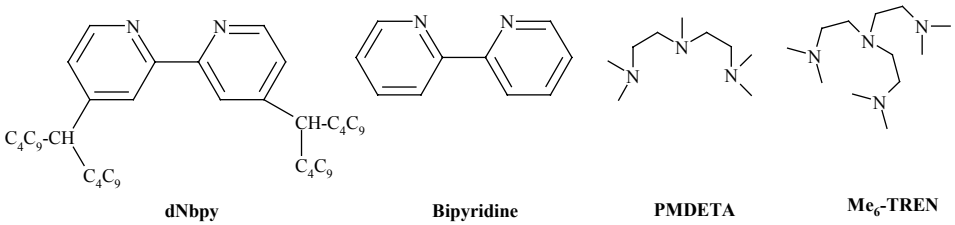

Figure 3. Examples of nitrogen-based ligands.

Iron is usually ligated by phosphine based ligands such as tributylphosphine or triphenylphosphine,[13,25] but can also be used in conjunction with nitrogen based ligands. Phosphorous-based ligands are also used to complex other metals in ATRP such as rhenium, ruthenium, rhodium, nickel and palladium.

Mechanism of ATRP

Controlled radical polymerization is based on the maintenance of a low, stationary concentration of the active species (free radicals) and the establishment of a fast, dynamic equilibrium between the active and dormant species.[49-50] In ATRP the active species is formed when the halogen in the alkyl halide is abstracted by the metal complex in a reversible redox process. This is illustrated in Figure 4. The bond between the alkyl and the halide is cleaved homolytically and a carbon-centered radical is formed on the alkyl.[2] In this process the deactivation rate must be higher than the activation rate in order to create a low concentration of propagating radicals. Thus, the equilibrium between active and dormant species must be greatly shifted towards the dormant species. If deactivation is very slow or non-existent the polymerization becomes uncontrolled.[33] The over-all rate of the reaction is highly dependent on the redox potential of the metal complexes.

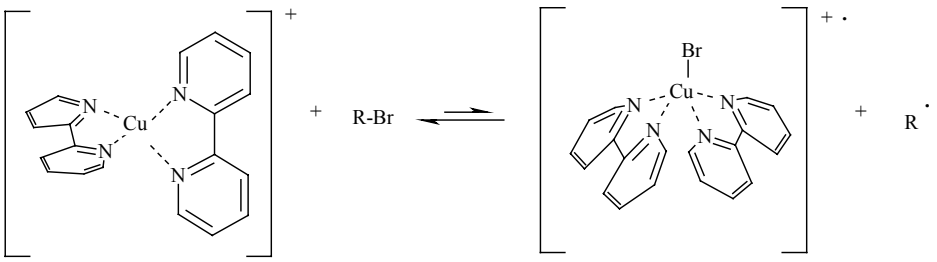

Figure 4. The metal complex exemplified with Cu(I) as the catalyst and Bipy as ligand.

The polymerization takes place in two steps: initiation and propagation. In Scheme 2 the mechanism is exemplified with copper as catalyst. Termination reactions also occur, but no more than a few percentages of the growing chains undergo termination in ATRP.[32]

Initiation

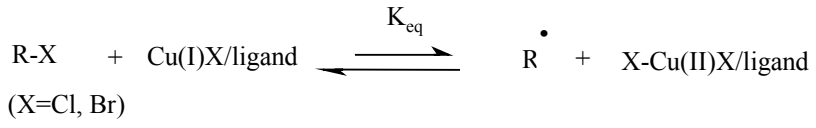

Propagation

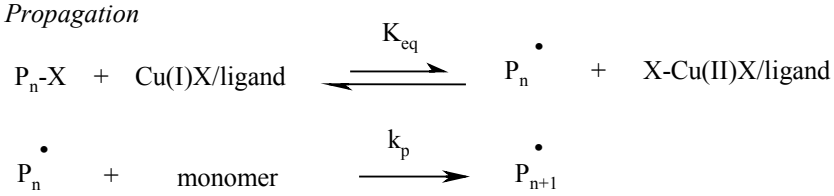

Termination

Scheme 2. The mechanism of ATRP.

From Scheme 2 the following rate laws are derived (equations 2 and 3):[10]

$$K_{eq} = \frac{k_{act}}{k_{deact}} = \frac{[P^{\bullet}][Cu(II)X]}{[Cu(I)][PX]} \tag{2}$$

$$R_p = k_p[P][M] = k_p K_{eq}[I]\frac{[Cu(I)X]}{[Cu(II)X_2]}[M] \tag{3}$$

Equation 3 is based on the assumption that the termination step can be neglected and that a fast pre-equilibrium is established. As can be seen, the propagation rate (R_p) of the polymerization is first order with respect to monomer concentration [M], initiator concentration [I] and activator concentration [Cu(I)X]. However, the reaction is not simply negative first order with respect to deactivator concentration [Cu(II)X_2]. This is due to the persistent radical effect, the irreversible formation of Cu(II)X_2 in the initial stages of the polymerization.[10]

HYPERBRANCHED POLYMERS

Polymerization of AB_x- type monomers yields polymers with a highly branched structure, Scheme 3. This group of polymers is called hyperbranched polymers or dendritic polymers. Dendritic polymers can be synthesized with most known polymer-forming reactions, such as condensation reactions,[51-53] cationic procedures,[51] ring-opening polymerization[54-57] and free radical procedures including controlled/"living" free radical polymerizations.[58-59]

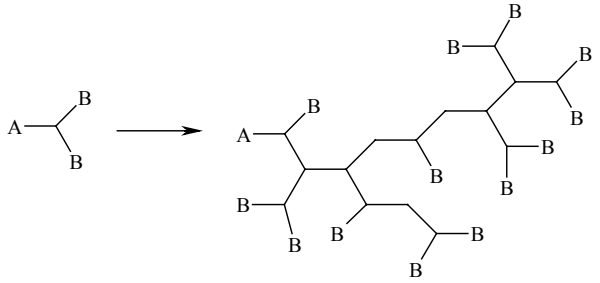

Scheme 3. Synthesis of hyperbranched polymers from AB_2-monomers.

The globular structure and the large number of end-groups give hyperbranched polymers unique properties.[60-62] The polymers do not entangle in the same degree as linear polymers, which greatly alters their mechanical and rheological properties compared to their linear analogues. The hyperbranched polymers have lower viscosity than their corresponding linear polymers with equal molecular weights.

Hyperbranched polymers as multifunctional initiators

The large number of end-groups of the hyperbranched polymer can be modified in several different ways. One way is to transform the end-groups into initiating groups for ATRP, Figure 5. The hyperbranched polymer then functions as a macroinitiator *i. e.* a multifunctional initiator, an initiator with more than one initiating group,[63-72] in the ATRP. This will yield polymers with a dendritic-linear architecture, having the hyperbranched part as a core with linear segments growing out from it. For example, Fréchet *et al.*[64] used isophthalate ester-functionalized dendrons featuring benzylic halide groups at their focal points for controlled radical polymerization of styrene, Haddleton *et al.*[63] used carbosilane dendritic initiators (**A** in Figure 5) for the polymerization of methyl methacrylate, Hedrick *et al.*[67] used dendritic polyester for the ATRP of methyl methacrylate (**B** in Figure 5) and Frey *et al.*[70] used a well-defined hyperbranched polyglycerol core for methyl acrylate. This combination of dendrimer synthesis and controlled radical polymerization is an interesting field that yields new polymeric materials.[63]

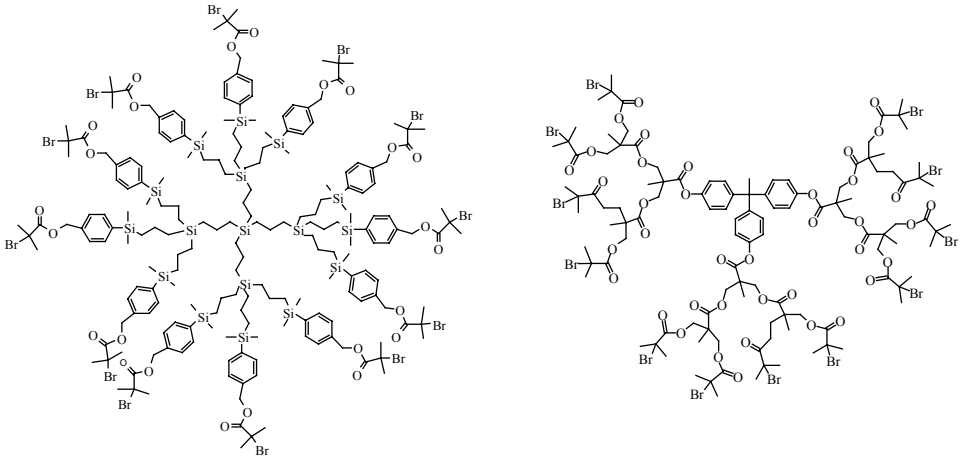

A **B**

Figure 5. Examples of dendritic structures where the end groups have been turned into initiating moieties for ATRP.

SYNTHESIS OF POLYMER BRUSHES FROM SOLID SUBSTRATES

Polymer chains can be attached to a solid surface, and then form so-called polymer brushes. The polymers can either be attached to the surface physically or chemically. Chemical attachment is usually preferred in order to avoid adhesion problems.[73] When the polymer is attached chemically it is covalently bonded to the surface. This can be accomplished in two ways, by "grafting to" (Figure 6) or "grafting from" (Figure 7).[74]

In the "grafting to" technique the polymer is pre-synthesized. It is end-functionalized in such a way that it will react with groups on the surface, hence attaching the entire arm of the polymer. The advantages with this technique are that the properties of the polymer brush easily can be tailored and that the polymer can be analyzed prior to attachment. However, only small amount of polymer can be immobilized onto the surface with this technique. As more chains become attached to the surface it gets more difficult for remaining chains to diffuse through the film and reach the reactive sites on the surface. Thus, only thin films can be formed (about 1-5 nm) and the brushes have a low grafting density.

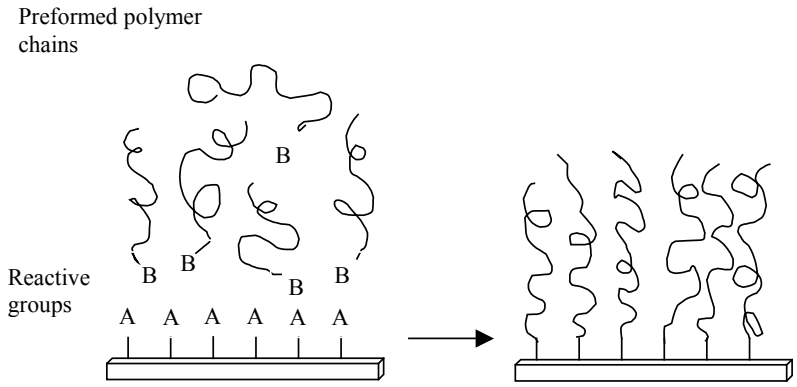

Figure 6. The "grafting to" technique with preformed, end-functionalized polymer.

In the "grafting from" technique initiating groups are immobilized on the surface, followed by polymerization from these groups, yielding polymer brushes. The attached polymer is more difficult to tailor this way, but much thicker films and higher grafting density can be obtained.

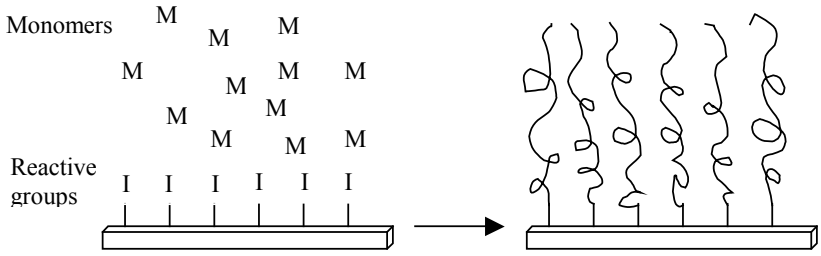

Figure 7. The "grafting from" technique with immobilized initiator groups.

ATRP from solid substrates

Solid substrates can also be used as multifunctional initiators in ATRP. If the groups on the surface are modified into initiating groups for ATRP, monomers can be grafted from the surface. ATRP has previously been utilized for "grafting from" processes from silicon,[75-79] gold[80-82] and silica[83] surfaces and from porous substrates.[84-85] Organic substrates have also been used, such as polystyrene latexes.[86-87]

One of the greatest advantages with using ATRP for "grafting from" is its ability to tailor the film thickness. It also offers control of the end-groups of the polymer on the surface and the surface can thereby be modified in different ways. Two main approaches have been used to control the growth of the polymer brushes. The first approach involves addition of sacrificial initiator to the reaction solution, thus forming a non-attached bulk

polymer. It is believed that the kinetics of the bulk reaction will be the same as the kinetics from the surface and that the grafted polymer will have essentially the same molecular weight as the one formed in bulk.[43-85] Hence, the ratio of the monomer/sacrificial initiator will also determine the DP for the grafted polymer. The second approach is to add excess deactivator (for example, $Cu(II)X_2$) to the reaction and not use a sacrificial initiator.[77] This way the only parameter that determines the film thickness is the reaction time.

When polymerizing from a surface the first step is to attach the initiator. In the case of gold and silicon surfaces this is accomplished by first forming a self-assembled monolayer (SAM) on the surface and then attaching the initiation moiety on the SAM.[73] On gold, for example, the most common route is to form a thiol bond between the gold and a hydroxy-functional thiol reactant, followed by reaction of the hydroxyl end-groups on the SAM with an acid halide, Figure 8. A disadvantage with this procedure is that the SAMs formed are thermally unstable at the elevated temperatures usually necessary for polymerization. ATRP at room temperature is always more desirable since it also suppresses the formation of thermally formed polymer.

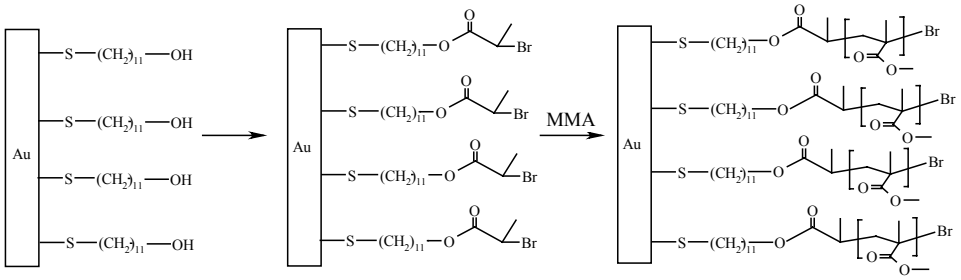

Figure 8. Modification of a gold surface into a multifunctional initiator for ATRP.

As mentioned previously, it has been suggested that the polymerization kinetics from the surface are the same as for ATRP in bulk. However, the close proximity of the growing chains, and hence the radicals, can cause an increased probability of radical-radical coupling. Therefore, termination reactions might be more profound in surface polymerization. The kinetics for ATRP from surfaces have not yet been thoroughly investigated.

CELLULOSE FIBERS

Cellulose is the major component in plants, such as wood and cotton. It is one of the most abundant renewable polymer resources. Cellulose is a natural polymer made up of β-1-4 D-glucose units, Figure 9.

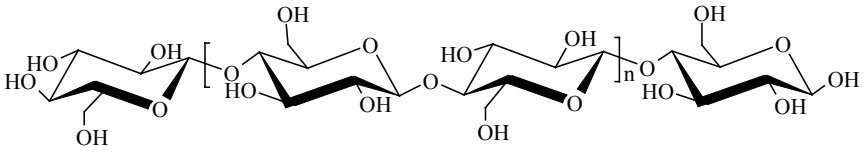

Figure 9. Repeating β-1-4 D-glucose units, structure of cellulose.

Due to the equatorial orientation of its many hydroxyl groups and to its linear structure, cellulose forms strong intermolecular and intramolecular hydrogen bonds. The intermolecular hydrogen bonds cause the natural cellulose to form a sheet-like structure and the polymer is crystalline.[88] The individual cellulose molecules form microfibrils, Figure 10. The microfibrils stack together and make up the fibrils, which gives the cellulose fibers. The polymer is very hydrophilic due to its many hydroxyl groups and it adsorbs water easily.

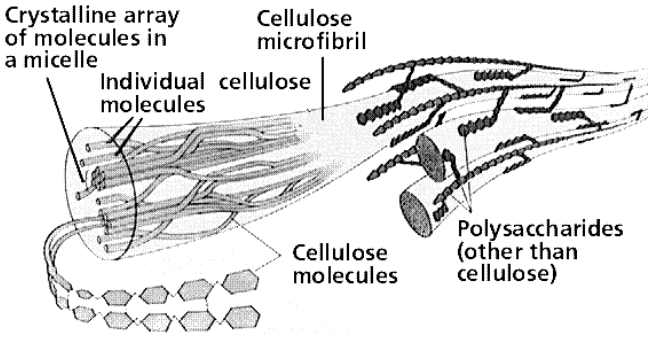

Figure 10. Structure of cellulose fibers.

Cellulose and its derivatives are found in a wide variety of applications such as fibers, plastics, coatings, films, wood and paper products. One of the uses of plant fibers is in high matrix composites. In these cases the fiber-to-matrix bonding needs to be optimized. This could be done by chemical modification of the fiber.

EXPERIMENTAL

MATERIALS

The hydroxy-functional polyoxetane was prepared as reported in the literature[54] from 3-ethyl-3-(hydroxymethyl)oxetane supplied from Perstorp AB, Figure 11. Tris(2-(dimethylamino)ethyl)amine (Me_6-TREN) was prepared similar to Ciampolini and Nardi[89] from tris(2-aminoethyl)amine (98%, Aldrich). Methyl acrylate, Cu(I)Br (Acros, 98%) and 2,2'-bipyridyl (Bipy, Acros, 99%) were used as received. 2-Hydroxyethylmethacrylate (HEMA, Aldrich, 97%) was purified immediately prior to use in order to remove impurities such as dimethacrylates and methacrylic acid, according to the following procedure: 50 ml of HEMA was dissolved in 150 ml of water. The water phase was extracted with 50 ml of hexane 10 times. 45 g NaCl was dissolved in the water phase. An organic layer was formed that was separated from the water phase. The organic phase was dried with $MgSO_4$, filtered and then passed over a column of aluminum oxide in order to remove the stabilizer. A filter paper, Whatman 1, was used as cellulose fibers. All other chemicals and solvents were used as received.

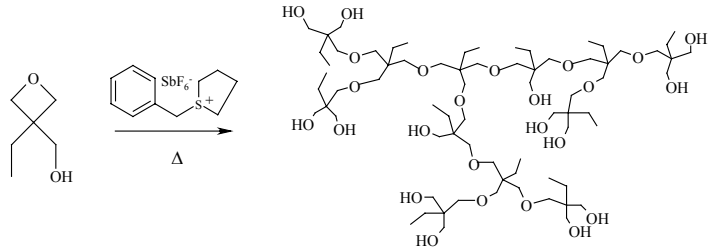

Figure 11. Polymerization of 3-ethyl-3-(hydroxymethyl)oxetane to give the hydroxy-functional hyperbranched polyoxetane.

APPARATUS

Infrared spectra were recorded on a Perkin-Elmer Spectrum 2000 FTIR equipped with a MKII Golden Gate™, Single Reflection ATR System from Specac Ltd, London, UK. The ATR-crystal was a MKII heated Diamond 45° ATR Top Plate.

^{1}H-NMR spectra were recorded on a 400 MHz Bruker Aspect NMR, using $CDCl_3$ as a solvent for PMA, Me_6-TREN and macroinitiator. DMSO-d_6 was used for PHEMA.

Molecular weights and polydispersities of methyl acrylate were determined by Size Exclusion Chromatography (SEC) on a Waters 717plus auto sampler and a Waters model 510 apparatus equipped with two PLgel 10 μm mixed-B columns, 300*7.5 mm (Polymer Labs., U.K.), with $CHCl_3$ as the mobile phase, 1 ml min^{-1}. Linear polystyrene standards were used for calibration, ranging from 1 700 to 706 000 g mol^{-1}.

Size exclusion chromatography (SEC) analyses of PHEMA were performed with a Waters 6000A pump, a PL-EMD 960 light scattering evaporate detector, two PL gel 10 μm mixed-B columns (300 x 7.5mm) from Polymer Labs and one Ultrahydrogel linear column (300 x 7.8mm) from Waters. All measurements were performed at 70°C. DMF was used as solvent at a flow rate of 1.0 ml min^{-1}. Linear polyethylene oxides were used for calibration.

Thermal analysis was performed on a Mettler DSC 820 calibrated according to standard procedures. Glass transition temperatures were determined as the inflexion points in the heat-flow curve from the second cooling. The analysis was carried out under nitrogen using a heating and cooling rate of 10 °C min^{-1}.

Electron Spectroscopy for Chemical Analysis (ESCA) spectra were recorded using a Kratos AXIS HS x-ray photoelectron spectrometer (Kratos Analytical, Manchester, UK). The samples were analyzed using a monochromator (Al x-ray source). The analysis area was below 1 mm^2.

Contact angle measurements were performed on a Ramé Hart goniometer. Deionized water (Millipore, resistivity: 18.4 MΩ cm) was used. The advancing contact angles were obtained by keeping the needle in the water droplet after positioning it on the surface and by carefully adding more water until the advancing angle appeared to be maximal. The measurements were performed with the needle remaining in the droplet.

POLYMERIZATION FROM POLY(3-ETHYL-3-(HYDROXYMETHYL) OXETANE)

Synthesis of macroinitiator

The macroinitiator was synthesized by reacting all the hydroxyl groups with 2-bromosisobutyryl bromide. This was done by first dissolving the polyoxetane in tetrahydrofuran (THF) prior to the reaction. N,N-dimethylaminopyridine (0.05 equiv. to hydroxyl groups in the polyoxetane) and triethylamine (1.1 equiv.) were then added. The flask was cooled in a water/ice bath. 2-Bromoisobutyryl bromide (1.0 equiv.) was diluted with THF and added drop-wise to the solution while stirring. The reaction was left to reach completion for approximately 24 hours. The solution was then precipitated in cold (-78°C) methanol. The residue was filtered and dried under vacuum. This yielded a colorless, sticky solid. The yield was rather low, approximately 25%. This was due to the sticky nature of the product, making work up procedures, such as filtration, difficult.

Polymerization from macroinitiator

Each polymerization was performed by essentially the same procedure. The ratio of initiating sites-to-monomer was varied in order to obtain different degrees of polymerizations (DP's). At the beginning of each reaction the macroinitiator was placed in a flask and dissolved in ethyl acetate (EtOAc, 33 w/w%). Methyl acrylate (MA), Me_6-TREN (0.05 equiv. to initiating groups) and Cu(I)Br (0.05 equiv.) were added and the flask was sealed with a rubber septum. The flask was evacuated and back-filled with Ar-gas three times. During this procedure a small amount of EtOAc and MA was evaporated, but since such large amounts of these two compounds were used in every polymerization it was found to be negligible. The degassing was performed for the same time period for each polymerization. The polymerization started immediately upon degassing and was left to proceed at room temperature. For conversion measurements samples were withdrawn with a syringe at time intervals. The withdrawn samples were analyzed with ^{1}H-NMR in $CDCl_3$, Figure 15b, without further purification. When the reaction was completed, the reaction mixture was diluted with THF and passed through a column of neutral aluminum oxide in order to remove most of the Cu-complex. The solvents and excess monomer were evaporated and the product was dried under vacuum. A pale green, sticky polymer was produced, colored by traces of copper.

POLYMERIZATION FROM CELLULOSE FIBERS

Immobilization of the initiator

The filter paper was washed with ethanol and dichloromethane prior to use. Ultrasonication was used for five minutes, with the paper immersed in dichloromethane. The hydroxyl groups on the surface was then reacted by immersing the paper in a solution containing 2-bromoisobutyrylbromide (50 mM), triethylamine (55 mM) and

catalytic amount of DMAP in CH_2Cl_2. The reaction was left to proceed at room temperature for 1-24 hours. The filter paper was thereafter thoroughly washed with dichloromethane and ethanol under ultrasonication

Grafting of the modified filter paper with methyl acrylate (MA)

The grafting was accomplished by immersing the initiator-modified paper into the reaction mixture containing MA, Cu(I)Br (0.01 equiv. to sacrificial initiator), Me_6-TREN (0.01 equiv.), sacrificial initiator (2-ethyl isobutyrylbromide, EBiB), and EtOAc (33 w/w%). The flask was sealed with a rubber septum, evacuated and back-filled with Ar-gas three times. The degassing was performed for the same time period for each polymerization. The polymerization started immediately upon degassing. All polymerizations were carried out at room temperature for 18 hours. After completed polymerization the papers were subjected to intense washing: THF, THF:water; water, and dichloromethane. Ultrasonication was used in combination with all four solvents. Finally, the paper was washed with dichloromethane for 48 hours, on a shaking device. No washing by solvent reflux was conducted in order to avoid heat treatment of the fibers. The bulk polymer was dissolved in THF and passed through a column of neutral aluminum oxide, in order to remove the copper complex. Ethyl acetate, MA and THF were evaporated until only the polymer remained.

Grafting of the PMA grafted cellulose fibers with 2-hydroxyethyl methacrylate (HEMA)

The reaction conditions for the polymerization of HEMA with ATRP were adopted from Matyjaszewski *et al*.[48] Cellulose fibers grafted with PMA (DP=200) were immersed into a solution of HEMA, EBiB, Cu(I)Cl, Bipy and MEK/1-propanol (30:70, 50 w/w %). The flask was sealed with a rubber septum and evacuated and back-filled with Ar-gas three times. The flask was immersed in a pre-heated oil bath, thermostated at 50°C. At the end of the reaction, the viscous mixture was dissolved in more solvent (MEK/1-propanol). The un-grafted polymer was precipitated in cold (-78°C) THF and filtered under vacuum. The grafted paper was washed thoroughly water and DMF, using ultrasound. The paper was left on a shaking device in DMF for 48 hours. In order to remove the DMF from the fiber, the paper was then left in water for 24 hours and then MeOH for another 24 hours.

RESULTS AND DISCUSSION

POLYMERIZATION FROM POLY(3-ETHYL-3-(HYDROXYMETHYL) OXETANE)

Synthesis of macroinitiator

The hydroxyl groups in the polyoxetane were reacted with 2-bromoisobutyryl bromide, yielding bromo-ester end-groups on the hyperbranched polymer, Figure 12. The resulting polymer was analyzed with SEC, ^{1}H-NMR, and FT-IR.

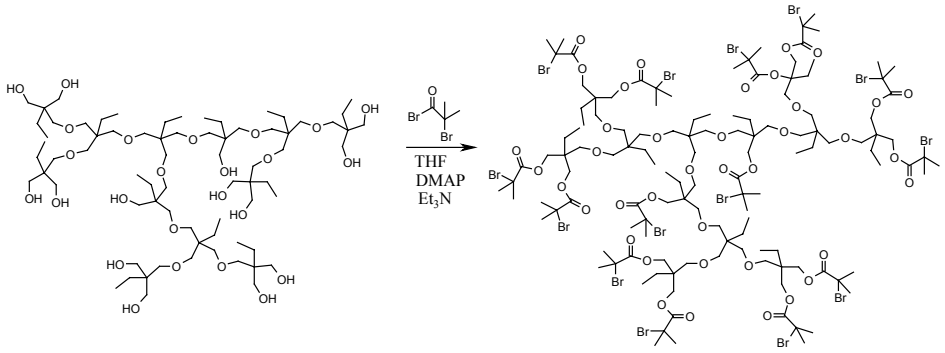

Figure 12. Reaction of poly(3-ethyl-3-(hydroxymethyl)oxetane) with 2-bromoisobutyryl bromide.

As can be seen from the FT-IR spectra of the macroinitiator and the polyether, Figure 13, the macroinitiator was successfully synthesized with complete conversion of the hydroxyl groups. The polyether shows a broad peak around 3300 cm^{-1}, originating from the OH-end group, which completely disappears after the reaction with 2-bromoisobutyryl bromide. The macroinitiator shows a peak around 1730 cm^{-1} which is not present in the polyether. This peak originates from the carbonyl in the bromo-ester group.

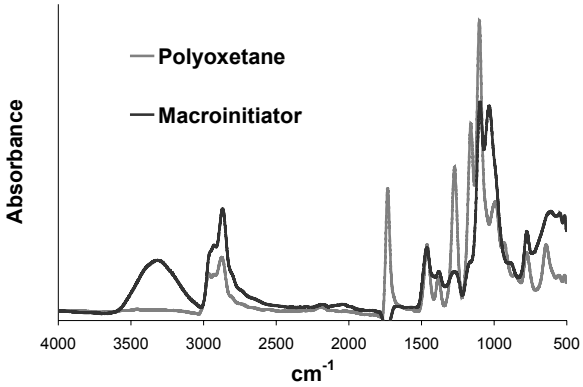

Figure 13. FT-IR of the polyoxetane and the macroinitiator.

^{1}H-NMR of the macroinitiator, with peak assignments, is shown in Figure 15a.

Polymerization from macroinitiator

There are several difficulties in using a multifunctional initiator instead of a monofunctional compound. Each molecule gives rise to a large number of growing chains and this causes an increased probability of intermolecular reactions. For example, Frey *et al.*[70] observed gelation after 35% monomer conversion when a multifunctional initiator was used for ATRP of MA in bulk. They attributed the gelation to coupling reactions between propagating radicals.

In order to prevent a polymerizing system from forming a gel, the concentration of propagating radicals has to be kept low. This can be accomplished in different ways. Diluted systems give a lower concentration of radicals. The system can be diluted either by adding a solvent or by quenching the reaction at very low conversion of the monomer, thus allowing the excess monomer to dilute the system. Another approach is to lower the amount of catalyst used, thus creating fewer radicals.

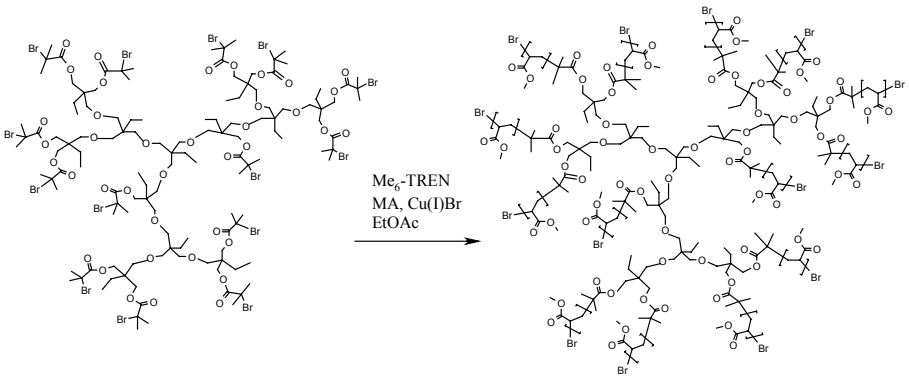

Figure 14. Polymerization of methyl acrylate from the macroinitiator.

The macroinitiator was used for the polymerization of methyl acrylate, Figure 14. The polymerization was performed at room temperature, mediated by Cu(I)Br and Me_6-TREN. Matyjaszewski *et al*. have shown that MA can be polymerized with ATRP at room temperature when using Me_6-TREN as a ligand in conjunction with Cu(I).[48] Polymerization proceeds quickly and the resulting PMA has very low polydispersity. Essentially the same reaction conditions were therefore chosen in this study. As can be seen in Table 1, methyl acrylate was successfully polymerized from the macroinitiator using Me_6-TREN as a ligand. The polymerization was fast at room temperature and yielded polymers with narrow polydispersities. The polymers were analyzed with SEC, ^{1}H-NMR and DSC.

Table 1. Results from SEC and the NMR analysis of the polymers.

No	[M]:[I]:[Cu(I)]:[L]	Time [min]	M_n[a] [g mol^{-1}]	PDI	DP (SEC)	DP (NMR)	M_n[b] [g mol^{-1}]
1	30:1:0.05:0.05	20	32 950	1.25	12	14	36 880
2	50:1:0.05:0.05	45	42 100	1.13	16	20	49 800
3	50:1:0.05:0.05	40	48 200	1.23	19	28	67 010
4	50:1:0.05:0.05	60	50 850	1.22	20	31	73 470
5	100:1:0.1:0.1	55	86 700	1.84	37	67	150 950
6	100:1:0.05:0.05	150	84 250	1.42	36	70	157 410
7	150:1:0.05:0.05	120	95 450	1.28	41	87	194 000

[a]Molecular weight measured by SEC
[b]Molecular weight calculated from ^{1}H-NMR

In this case the polymerization had to be performed in ethyl acetate since the attempted bulk polymerizations resulted in polymers with high polydispersity. Molecular weights and polydispersities were determined by Size Exclusion Chromatography, using linear polystyrene standards. The obtained molecular weights are probably much lower than the actual values since highly branched polymers are known to have smaller hydrodynamic volume than their linear analogues.[67] The M_n has therefore also been calculated from ^{1}H-NMR. The determined polydispersity values might not agree completely with the real values since hybrid dendritic-linear polymers are analyzed.

When a ratio of initiating sites-to-catalyst of 1:0.05 was used the polymers from all the reactions had a low polydispersity, ranging from 1.1-1.4, indicating a well-controlled polymerization. The SEC curves of the polymers were narrow and monomodal. When the ratio of initiating sites-to-catalyst was raised to 1:0.1 there was a sudden increase in the polydispersity, which shows a lack of control over the polymerization at this concentration of radicals.

In order to obtain different degrees of polymerization (DP), the ratio of monomer-to-initiating sites was varied. The DP was calculated both from SEC and from ^{1}H-NMR. When calculating the DP from SEC the assumption was made that the macroinitiator had 25 initiating sites and that each initiating site gave rise to one polymer arm.

a)

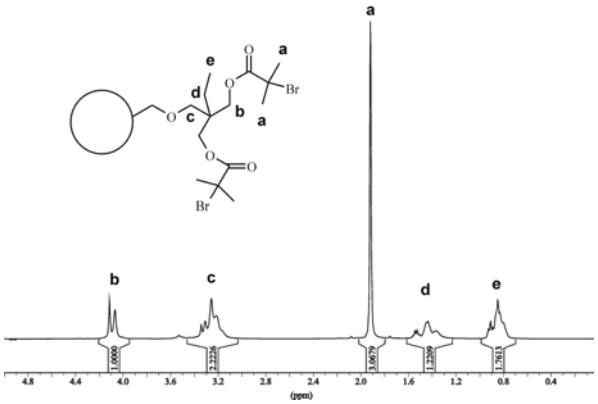

b)

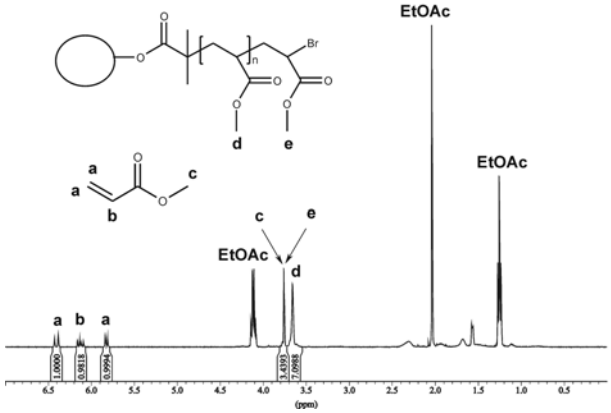

c)

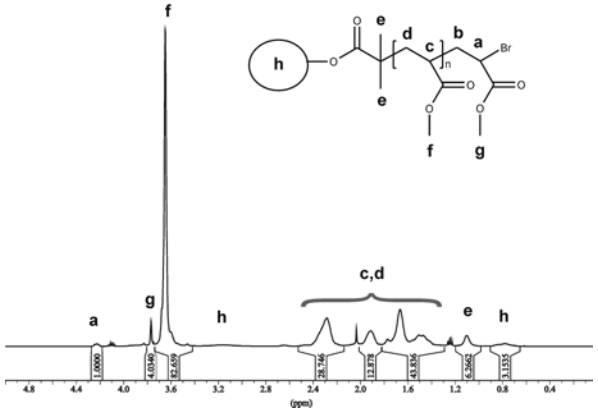

Figure 15. a) ^{1}H-NMR (in $CDCl_3$) and peak assignments of the macroinitiator. b) ^{1}H-NMR (in $CDCl_3$) and peak assignments of the reaction mixture, containing monomer, polymer and EtOAc. c) ^{1}H-NMR (in $CDCl_3$) and peak assignments of the resulting polymer, with traces of EtOAc remaining.

When calculating the DP of the PMA arms in the hybrid dendritic–linear molecule the molecular weight of the macroinitiator was 6750 g mol^{-1}, as determined by SEC. Figure 15c shows an example of ^{1}H-NMR of a resulting polymer, entry 3 in Table 1. From ^{1}H-NMR the DP was calculated by adding the integrals from the peaks of all the methyl groups (3 H) in the polymer (assigned **g** and **f** in Figure 15c) and dividing the sum with half of the integral from the peak of the methyl groups (6 H) in the macroinitiator (assigned **e** in Figure 15c). Another way of calculating the DP is to divide the sum of the integral from **f** and **g** in Figure 15c with the integral from **a** taken three times. In Figure 15c these two methods both give a DP of 28. A third way is to divide the sum of the integrals from all the methyl groups in the polymer (**f** and **g** in Figure 15c) with the integral from the terminal methyl groups in the chain (**g** in Figure 15c). However, the peaks **f** and **g** in Figure 15c are poorly separated and this calculation should only be considered as a rough estimation. As expected, the DP's calculated from SEC are lower than the DP's calculated from ^{1}H-NMR. The difference between the two values increases with increasing molecular weight.

The monomer conversion can be calculated from ^{1}H-NMR of the crude product. An example of this can be seen in Figure 15b where conversion is calculated by dividing the integral from the peak from the methyl group in the chain (denoted **d** in Figure 15b) with the sum of the integral from all the methyl groups in both the monomer and the polymer chain (denoted **c**, **d** and **e**). From Figure 15b it can be calculated that the overall conversion in this reaction was about 65%.

Kinetic experiments show that the reaction rate rapidly decreases around 70-80% conversion and that longer reaction times do not give an increase in conversion. This is suggested to be due to the persistent radical effect, converting the catalyst irreversibly from Cu(I) to Cu(II). This indicates that side reactions begin to take place at higher conversions, which results in an increase in the polydispersity index. The increase is rather small but this could be attributed to the fact that the initial concentration of Cu(I) is very low and only a few side reactions need to take place to convert all the Cu(I) to Cu(II). It is hypothesized not to give rise to a large change in the polydispersity.

As can be seen in Figure 15a the ratio of the integral originating from the methyl groups (6 H) in the bromo-ester (denoted **a** in Figure 15a) and the integral from the methyl groups (3 H) originating from the polyether (denoted **e** in Figure 15a) should be about 2:1. The methyl groups from the bromo-esters will shift from about 1.9 ppm in the macroinitiator to about 1.1 ppm in the co-polymer. If all the initiating sites in the macroinitiator initiate polymerization the ratio of the integral from this shifted peak (denoted **e** in Figure 15c) and the integral from the methyl groups originating from the polyether (denoted **h** in Figure 15c) should remain the same, about 2:1. As can be seen in Figure 15c, this is the case. The peak from the macroinitiator is, however, very small and the integral can only be determined roughly, and it is therefore difficult to confirm if all the initiating sites are active.

The relationship between peak **a** (originating from the proton alpha to the bromide in each chain end) and peak **e** should be 1:6. This is clearly the case in the spectrum, which

shows that there has been essentially no loss of the bromide atom at the chain ends, hence the reaction is "living". This is further evidence of the controlled nature of the polymerization and shows that side reactions, such as termination, have been suppressed.

Table 2. Thermal analysis of the polymerized macroinitiator.

No.	DP_{sec}	T_g^1 [°C]	T_g^2 [°C]
1	12	≈ -40	3
2	19	≈ -40	6
3	36	≈ -40	12

The PMA-grafted polymers exhibited two glass transitions, T_g's, (Table 2 and Figure 16) in differential scanning calorimetry (DSC), indicating that the resulting block-copolymers are phase-separated. The lower glass transition (approx. -40°C) is unaffected by the length of the PMA grafts and therefore assumed to originate from the hyperbranched polyether core. The hyperbranched polyether could be compared to poly(ethylene oxide) (PEO), which is a linear polyether that has a T_g of -60°C. In contrast, the higher glass transition is affected by the length of the grafts and therefore suggested to originate from the poly(methyl acrylate) grafts. According to literature data the T_g of free PMA should be around 6-9°C.[90]

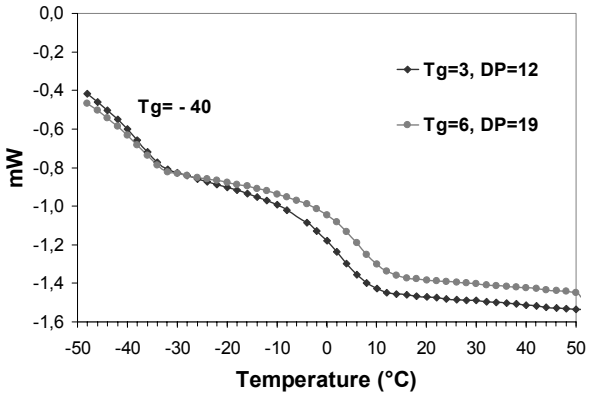

Figure 16. DSC traces of the resulting polymer (entries 1 and 3 in Table 1).

POLYMERIZATION FROM CELLULOSE FIBERS

ATRP has been performed from surfaces such as gold, silicon and silica particles. Only a few examples are found in the literature of grafting with ATRP from organic substrates. This study reports on the first grafting of a naturally occurring polymer, cellulose fibers with ATRP. A filter paper was chosen for cellulose fibers. This was done in order to avoid problems with free fibers and simplify work-up procedures. The filter paper of choice was Whatman 1, due to its high cellulose content and low amount of impurities.

Immobilization of the initiator

The hydroxyl groups on the filter paper surface were reacted with 2-bromoisobutyryl bromide, yielding bromo-ester groups on the surface that are known to be good initiators for ATRP, Figure 17.

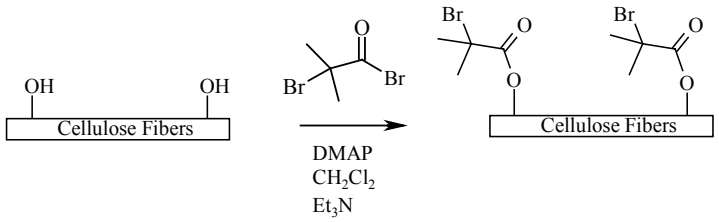

Figure 17. Immobilization of initiator on the cellulose fibers.

An attempt was made to analyze the initiator modified cellulose fibers with FT-IR, DSC and contact angle measurements. However, the content of bromo-ester groups at the surface was too small to enable measurement with FT-IR and DSC and no difference between virgin and modified filter paper could be detected. The water adsorption ability on the surface had noticeable decreased but no contact angle could be measured since the papers rather rapidly adsorbed water. The bromo-content on the surface was only detectable with ESCA. The cellulose fibers were subjected to the reaction solution containing 2-bromoisobutyryl bromide for different time periods, 1, 2, 6, 18 and 24 hours.

Table 3. ESCA analysis of initiated filter paper.

Reaction time [h]	Mass % C	Mass % O	Mass % Br
1	51.7	46.6	1.70
2	52.6	46.0	1.4
6	51.3	46.4	1.9
18	51.1	44.5	4.3
24	49.4	47.6	3.1

From ESCA analysis it could be concluded that the reaction time was crucial for the amount of initiator that was immobilized onto the surface. The bromo-content on the surface increased with increasing reaction time, up until 18 hours, Table 3.

Figures 18 and 19 show the peaks from the bromide in ESCA. The baseline becomes quite noisy, especially for those surfaces with the lowest bromo-content, Figure 18. Due to this, evaluation of these curves is difficult. The values in Table 3 should therefore only be considered as rough estimations of the bromo-content on the surfaces, and not as absolute values.

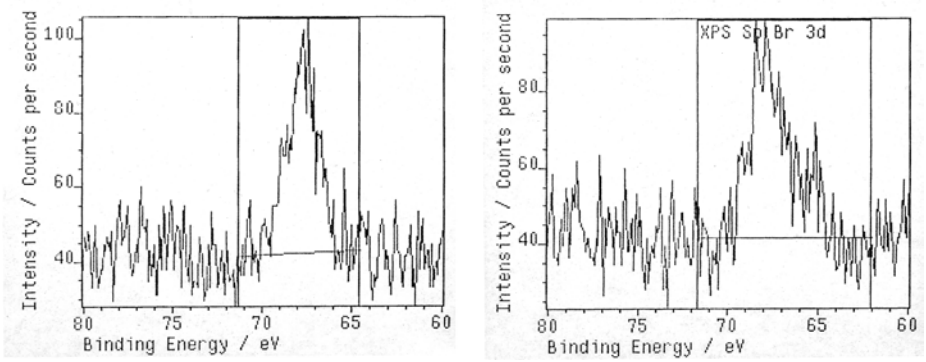

Figure 18. Spectra of the bromide peak in ESCA for R_T= 1 h (left spectrum) and R_T=6 h (right spectrum).

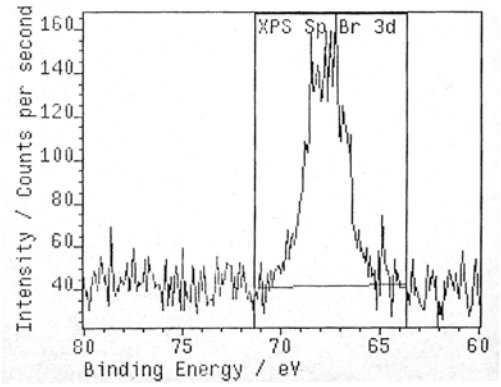

Figure 19. Spectrum of the bromide peak in ESCA for R_T=18 h.

Grafting of the modified filter paper with methyl acrylate

The grafting of PMA was performed on papers that had been reacted with 2-bromoisobutyryl bromide for 24 hours, Figure 20. The polymerization was conducted in ethyl acetate in order to simplify the work up of the product. The reaction conditions were mainly adopted from Matyjaszewski *et al.*[48] who showed that ATRP of MA at room

temperature with Me_6-TREN yielded PMA with very low polydispersities. Similar conditions were used as Baker *et al.*[81] when polymerizing MMA from gold surfaces at room temperature.

Since the number of initiating sites on the surfaces was unknown a sacrificial initiator, ethyl 2-bromoisobutyrate, was added in order to control the length of the PMA-grafts, as the ratio between the free initiator and monomer determines the degree of polymerization. In this study DP's of 100, 200 and 300 were attempted.

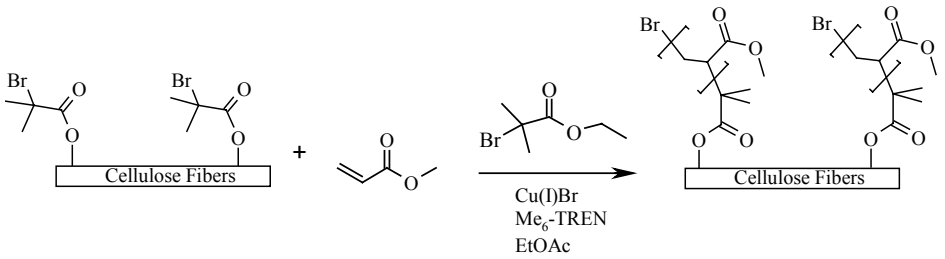

Figure 20. Polymerization of MA from initiator-immobilized cellulose fibers.

In order to verify that the polymer on the surface was covalently bonded and not just physiosorbed, a blind test was performed (denoted blank in Table 4 and Figure 19). This sample was treated identically to the samples subjected to polymerization with the exception that no initiator was immobilized on its surface prior to being subjected to the polymerization solution. The aimed DP for this sample (the bulk polymer) was 200.

Table 4. Results from SEC and Contact Angle Measurements.

Sample (DP aim)	M_n theor.	M_n	DP*)	PDI	Contact Angle, $(\theta)_a$
blank	17,212	14,830	172	1.05	-
DP-100	8,609	6,430	75	1.10	-
DP-200	17,212	12,810	149	1.06	128±10º
DP-300	25,818	25,630	298	1.05	133±5º

**) The degree of polymerization was calculated from SEC data.*

The non-immobilized polymers were analyzed with SEC, Table 4. All the polymerizations proceeded in a controlled manner, yielding PMA with very low polydispersities, below 1.1. The targeted DP's deviates somewhat from the measured ones indicating that the reaction conditions are not optimized.

The roughness of the filter paper surface makes surface characterization of the modified cellulose fibers difficult. It renders ellipsometry impossible and contact angle measurements problematical. The values of the contact angle measurements in Table 4 should therefore only be considered as a rough estimation. For that reason only the advancing angle, $(\theta)_a$, has been measured. The contact angle measurements do show,

however, that the surface becomes increasingly hydrophobic with increasing DP of the grafted PMA arms. Samples DP-200 and DP-300 were very hydrophobic and no adsorption of water could be detected. For sample DP-100 no contact angle could be measured since the paper slowly adsorbed water. The blank sample quickly adsorbed water and behaved just like the virgin filter paper with respect to water adsorption. This indicates that the hydrophobicity of samples DP-200 and DP-300 originates from grafted PMA and not just physiosorbed polymer.

The grafted and un-grafted filter papers were also analyzed by FT-IR. Figure 21 shows the carbonyl absorbance at 1730 cm^{-1}. A clear difference can be seen in the carbonyl content on papers with different DP's. As can be seen in the curve denoted "filter paper", that originates from virgin filter paper only subjected to solvents and MA, there are no carbonyls present in the cellulose fiber structure. Hence, this peak in the other samples only originates from the carbonyl in PMA. It is clearly seen that the amount of PMA grafted on the surface increases almost proportionally with graft length of the bulk polymer. This indicates that the thickness of the grafted layer can be tailored by altering the monomer-to-sacrificial initiator ratio. Furthermore, this implies that the polymer graft-lengths on the surface can be controlled by ATRP.

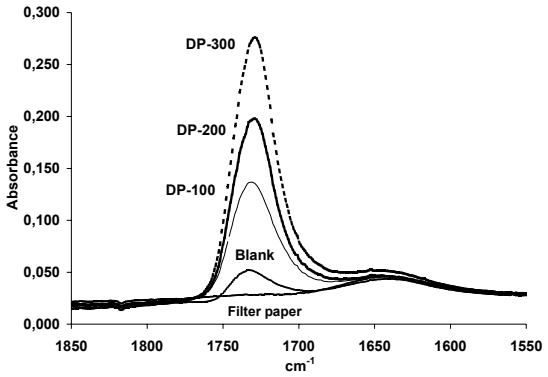

Figure 21. The carbonyl absorbance in FT-IR of grafted and un-grafted filter paper.

FT-IR analysis of the blank filter paper revealed a small carbonyl peak, which is attributed to physiosorbed PMA. This implies that the washing procedure was not completely successful. Most likely, all grafted surfaces contain some physiosorbed PMA. However, the difference between the grafted samples and the blank is still evident.

In order to verify that the polymerization from the surface is controlled, it is desirable to cleave off the PMA grafts and analyze them separately with SEC. This was attempted and the grafts were cleaved from the cellulose fiber with hydrolysis (KOH/MeOH). Unfortunately the small amount of grafted PMA on the surface made work-up procedures impossible and the polymers could not be detected after cleavage. Attempts were made to grow higher DP's in order to increase the amount of PMA on the surface, but increasing the targeted DP(>600) broke down the cellulose structure. This could be explained by the fact that the cellulose structure is held together by hydrogen bonds. When a substantial

amount of the hydroxyl groups are reacted, the intermolecular bonds weaken and this causes the cellulose structure to deteriorate at high DP's.

The grafted filter paper was also analyzed by ESCA. However, no bromo-content could be detected on the surface. This is probably due to the ESCA method, which only measures depths of 2-10 nm. The chains on the surface could exhibit an entangled behavior and the chain-ends might therefore not be situated directly in the outermost layer. Another explanation is, of course, that termination reactions have taken place to a large extent on the surface, and the chain ends are "dead".

DSC analysis of the grafted filter paper showed no transition for DP-100, Figure 22. However, DP-200 and DP-300 showed a transition around 15-20°C, the transition being larger for DP-300 than DP-200, indicating that more polymer has been attached on sample DP-300 than DP-200.

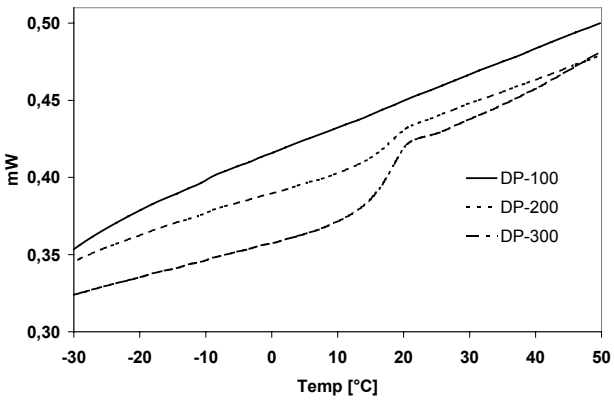

Figure 22. DSC of the grafted filter paper.

Grafting was also accomplished on the paper that had been reacted with 2-bromoisobutyryl bromide for different periods of time, 1 h, 6 h and 18 h. The targeted DP of these grafts was 200 for all three samples. The results from the SEC analysis are shown in Table 5.

Table 5. SEC analysis of the bulk polymer.

Sample	M_n theor.	M_n	DP*)	PDI
R_T= 1h	17,212	16,740	194	1.12
R_T= 6 h	17,212	15,190	176	1.14
R_T= 18 h	17,212	18,710	217	1.11

**) The degree of polymerization was calculated from SEC data.*

Contact angle analysis showed that all the papers were hydrophobic and did not absorb water. FT-IR analysis shows an increase in carbonyl content with increasing reaction time of the immobilization of the initiator, Figure 23. ESCA analysis showed a rather small increase in bromo content on the surface between R_T=1 and R_T=6 h after immobilization of initiator (Table 3 and Figure 18), but the increase in the carbonyl peak after grafting of PMA is quite large. ESCA analysis also showed that R_T=6 h and R_T=18 had a significant difference in bromo-content on the surface after immobilization of initiator (Table 3, Figures 18 and 19). However, the increase in carbonyl content between these two samples is smaller compared to the increase between R_T=1 h and R_T=6 h. One explanation for this could be that not all the bromo-ester groups in R_T=18 h are accessible for polymerization. Another explanation could be that the chains in R_T=18 h grow closely together and due to this are more probable to terminate. Also, the bromo-content on all the papers after immobilization of initiator is low, and the peak from bromide is hard to evaluate, as was discussed previously. The noise levels are quite high, especially in the papers with the shortest reaction times for immobilization of initiator (Figure 18 and 19). It might be that the difference in bromo-content between R_T=1 h and R_T= 6 h is bigger than the values in Table 3 indicates. Other factors, such as impurities and the fact that the bromide might not be situated directly on top of the surface, also affect the results from the ESCA, and could explain the results from the FT-IR in Figure 23.

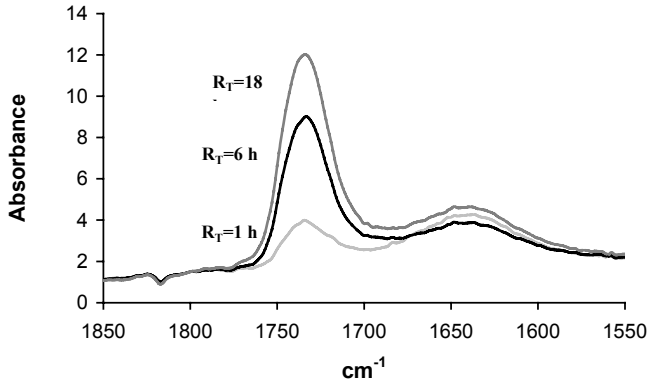

Figure 23. The carbonyl absorbance in FT-IR analysis of PMA grafted filter paper with different reaction times for the immobilization of initiator.

Grafting of the PMA grafted cellulose fibers with 2-hydroxyethyl methacrylate (HEMA)

If ATRP of PMA from cellulose fibers is controlled then the bromides at the chain ends should not be lost and can therefore work as an initiator for further polymerization. In order to verify this "livingness" of the grafted PMA layer, attempts were made to graft a layer of PHEMA on top of the PMA, creating a block co-polymer on the surface, Figure 24. The results herein only reports some very prelimiary results.

The grafting was accomplished on papers R_T=1 h, R_T=6 h and R_T=18 h. In order to control the washing procedure of the PHEMA grafted paper a blind test was performed.

This was done by immersing a virgin filter paper into a reaction solution and after polymerization washing the paper in the same way as the grafted ones.

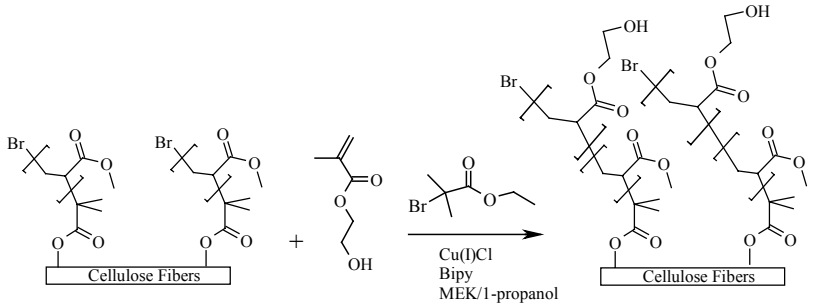

Figure 24. Polymerization of HEMA from PMA grafted cellulose fibers.

Since the polymerization took place in an oil bath stirring had to be accomplished with a magnetic bar. To avoid damaging the fibers, the paper was hung up on a polyethylene string, and the top part of the paper was not subjected to the reaction solution.

The non-immobilized PHEMA was analyzed with SEC. DP's of 200, 400 and 600 were targeted for paper R_T=1 h, R_T=6 h and R_T= 18 h respectively. However, SEC analysis shows that all the polymers had a DP of about 200. The peaks show a slight high molecular weight shoulder and have broader polydispersities. The reasons for this could be insufficient purification of the HEMA or that thermal polymerization has started to take place either before or during the ATRP. Impurities such as dimethacrylates will give rise to branching in the polymerization and this will yield polymers with higher polydispersity.

FT-IR of the block co-polymer grafted filter paper showed an increase in carbonyl content as the peak at 1730 cm^{-1} was enlarged compared to before the HEMA grafting, Figures 25-27. Interestingly, this increase is larger for the paper that has been reacted with 2-bromoisobutyryl bromide for the shortest time, R_T=1 h, and smallest for the paper that has been reacted for the longest time, R_T=18 h. This further strengthens the argument that more chains have been terminated on the surface with the highest amount of initiating sites. It is also possible that steric reasons make polymerization from the more crowded surface slower. FT-IR of the blank sample did not reveal any carbonyl content, indicating that the washing procedure for these papers was sufficient and than PHEMA was covalently bonded to the surface and not just physiosorbed.

No contact angles could be measured after the PHEMA grafting, since the polymer grafted papers slowly adsorbed water. Paper R_T=1 h adsorbed water very quickly while paper R_T=18 h adsorbed water much more slowly. It could be concluded that the hydrophobic behavior of the surface had changed after grafting of PHEMA and it was evident that the polymer layer behaved differently than prior to PHEMA grafting.

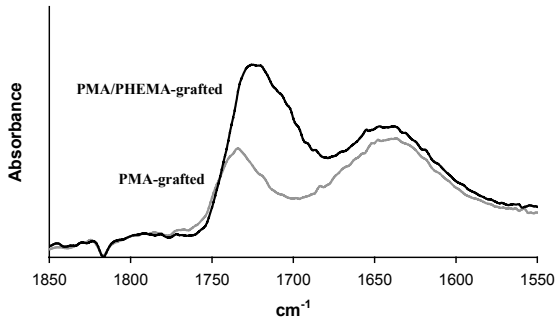

Figure 25. FT-IR of PMA grafted filter paper, R_T=1 h, before and after grafting of PHEMA.

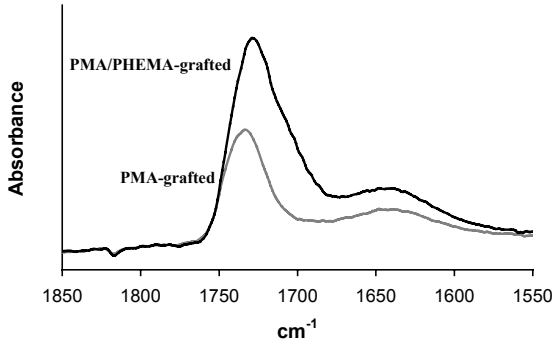

Figure 26. FT-IR of PMA grafted filter paper, R_T=6 h, before and after grafting of PHEMA.

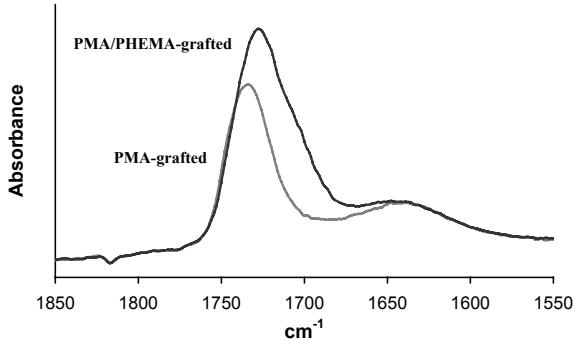

Figure 27. FT-IR of PMA grafted filter paper, R_T=18 H, before and after grafting of PHEMA.

CONCLUSIONS

Atom transfer radical polymerization (ATRP) of methyl acrylate has successfully been perfomred from two new multifunctional substrates.

A soluble multifunctional substrate has been synthesized by reacting poly(3-ethyl-3-(hydroxymethyl)oxetane) with 2-bromoisobutyryl bromide. The resulting macroinitiator had approximately 25 initiating sites. ATRP of methyl acrylate from the macroinitiator yielded polymers with a linear-dendritic architecture. Polymerization proceeded fast at room-temperature when Me_6-TREN was used as a ligand in conjunction with Cu(I)Br. The system showed good control and conversions as high as 65% were reached. The resulting polymers had low polydispersities (1.1-1.4) and the molecular weight could be tailored by altering the monomer-to-initiating sites ratio. ^{1}H-NMR analysis indicated that all the initiating sites had generated polymer chains.

An insoluble multifunctional substrate has been synthesized by reacting a filter paper with 2-bromoisobutyryl bromide. The cellulose fibers have successfully been grafted with PMA using ATRP, mediated by Me_6-TREN and Cu(I)Br. The polymerization proceeded in a controlled manner at room temperature. The resulting polymer-grafted papers were extremely hydrophobic, with contact angles larger than 100°. FT-IR analysis clearly showed that the graft length could be accurately controlled by altering the sacrificial initiator-to-monomer ratio. From ESCA analysis it could be concluded that the reaction time for the immobilization of the initiator was crucial for the number of initiating groups that was attached onto the surface, and hence for the resulting polymer layer. A second layer of PHEMA could be grafted onto the first PMA layer, showing that the chains on the surface has not been terminated to a great extent and that grafting under these conditions are “living”. Following grafting of HEMA the papers slowly absorbed water and it was evident that the hydrophobic behavior of the fibers had changed.

SUGGESTIONS OF FURTHER WORK

The modification of cellulose fibers with controlled/"radical" polymerization techniques is an interesting field that might yield new and improved applications for cellulose. However, the reaction conditions and work-up procedures need to be improved. In order to investigate the polymerization from the surface, and conclude that it is controlled, it is necessary to detach the polymer from the surface and analyze it separately. The kinetics of the surface polymerization is so far unknown and detachment of the polymer grafts would be one way to investigate this.

The versatility of the grafting process will be further investigated by the use of various monomers such as styrene, acryl amide and various dendritic monomers. Ideally, the surface properties of the fibers can be tailored by the appropriate choice of monomers. Eventually, surface-modified fibers could be used in composites.

The grafted fibers should be analyzed with other methods. For example, it could be interesting to investigate the barrier properties of the grafted fibers.

Since 2-bromoisobutyryl bromide is a very reactive and poisonous compound it would be desirable to immobilize initiating groups onto the surface through other techniques. Compounds such as xyloglucan, which contains a binding site that absorbs well to the cellulose, can be modified with an initiating moiety. Grafting can then be accomplished from the modified xyloglucan.

Instead of grafting an entire surface, the grafts can be ordered, yielding patterned surfaces. This can be done by micro contact printing of the initiator on substrates such as gold or silicon.

ACKNOWLEDGMENTS

First of all, my deepest gratitude goes out to my supervisor, Associate Professor Eva Malmström Jonsson, for accepting me as her graduate student, for her enthusiasm and bright ideas, but most of all for being such a good friend and wonderful person. I would also like to thank Professor Anders Hult for trying to keep "Ytbehandlingsgruppen" out of trouble and Associate Professor Mats Johansson for helping whenever help is needed, especially with the IR.

All the other colleagues and friends at the Department of Polymer Technology are thanked for creating a great atmosphere. The administrative personnel are thanked for all their help, especially Margareta Andersson, Ove Källberg and Inger Lord. Special thanks to Anna Finne for her work with the $CHCl_3$-GPC and Björn Olander for the ESCA measurements and evaluations. I would also like to thank Linda Sundberg for introducing me to the field of surface chemistry.

I would like to thank Dr. Ronnie Palmgren, Dr. Phillipe Busson, Dr. Michael Morrison and Associate Professor Mats Jonsson for valuable discussions concerning ATRP.

Sofia Söderberg is thanked for being a great diploma worker and for the contributions she has made to this thesis.

The Swedish Foundation for Strategic Research and the Swedish Research Council are gratefully acknowledged for financial support.

I would like to thank all the former and the present members of "Ytbehandlingsgruppen", especially my "roomies" Johan and Daniel for throwing stuffed animals at me and letting me keep them (the stuffed animals that is) hostage. All of ABB is thanked for great and insane times, especially Micke Krook who will never beat me at "Tequilabrottning".

Fredrik (*Fredan*) von Kieseritzky is thanked for always helping me with chemistry and for reminding me that I am only a "polymerare" and not a real chemist. You are a true friend!

All my friends outside the department, especially Challe, Erica, Fille, Katha, Kathies, Johan, Lena and Mickan are thanked for being such a great bunch of people and for being my friends even at times when I don't deserve it.

I am forever grateful to my family, especially my mother Barbro, my father Karl and my little brother Johan, for believing in me and loving me and for giving me the freedom to make my own choices, however crazy they might think I am.

Finally I would like to thank Per, who in such a short time has become the most important part of my life. Now I can't imagine it without you!

REFERENCES

1. Wang J.-S.; Matyjaszewski K. *J. Am. Chem. Soc.*, **1995**, *117*, 5614-5615.
2. Wang J.-S.; Matyjaszewski K. *Macromolecules,* **1995**, *28*, 7901-7910.
3. Kato M.; Kamigaito M.; Sawamoto M.; Higashimura T. *Macromolecules,* **1995**, *28*, 1721-1723.
4. Boutevin B. *J. Polym. Sci., Part A: Polym. Chem*, **2000**, *38*, 3235-3243.
5. Curran D. P. *Synthesis*, **1988**, 489-513.
6. Karasch M. S.; Jensen E. V.; Urry W. H. *Science*, **1945**, *102*, 128.
7. Karasch M. S.; Skell P. S.; Fischer P. *J. Am. Chem. Soc*., **1948**, 1055-1059.
8. Patten T. E.; Xia J.; Abernathy T.; Matyjaszewski K. *Science*, **1996**, *272*, 866-868.
9. Patten T.; Matyjaszewski K. *Adv. Mater.,* **1998**, *10*, 901-915.
10. Matyjaszewski K.; Patten T. E.; Xia J. *J. Am. Chem. Soc.,* **1997**, *119*, 674-680.
11. Kotani Y.; Kamigaito M.; Sawamoto M. *Macromolecules,* **2000**, *33*, 6746-6751.
12. Percec V.; Barboiu B. *Macromolecules*, **1995**, *28*, 7970-7972.
13. Matyjazsewski K.; Wei M.; Xia, J.; McDermott N. E. *Macromolecules*, **1997**, *30*, 8161-8164
14. Davis K. A.; Paik H.-j.; Matyjaszewski K. *Macromolecules*, **1999**, *32*, 1767-1776.
15. Coca, S.; Jasieczek C. B.; Beers K. L.; Maytjaszewski K. *J. Polym. Sci., Part A: Polym. Chem.,* **1998**, *36*, 1417-1424?
16. Mühlebacj A.; Gaynor S. G.; Matyjaszewski K. *Macromolecules*, **1998**, *31*, 6046-6052.
17. Moineau G.; Minet M.; Dubois Ph.; Teyssié Ph.; Senninger T.; Jérôme R. *Macromolecules*, **1999**, *32*, 27-35.
18. Davis K. A.; Matyjaszewski K. *Macromolecules*, **2000**, *33*, 4039-4047.
19. Wang J.-L.; Grimaud T.; Matyjaszewski K. *Macromolecules*, **1997**, *30*, 6507-6512.
20. Haddleton D. M.; Clark A. J.; Crossman M. C.; Heming A. M.; Morsley S. R.; Shooter A. J. *Chem. Commun.*, **1997**, 1173-1174.
21. Wang X.-S.; Lascelles S. F.; Jackson R. A.; Armes S. P. *Chem. Commun.*, **1999**, 1817-1818.
22. Johnson R. M.; Ng C.; Samson C. C. M.; Fraser C. L. *Macromolecules*, **2000**, *33*, 8618-8628.
23. Granel C.; Dubois Ph. Jérôme; Teyssié Ph. *Macromolecules*, **1996**, *29*, 8576-8582.
24. Grimaud T.; Matyjaszewski K. *Macromolecules*, **1997**, *30*, 2216-2219.
25. Ando T.; Kamigaito M.; Sawamoto M. *Macromolecules*, **1997**, *30*, 4507-4510.

26. Beers K. L.; Boo, S.; Gaynor S. G.; Matyjaszewski K. *Macromolecules,* **1999**, *32*, 5772-5776.
27. Matyjaszewski K.; Jo S. M.; Paik H.-j.; Gaynor S. G. *Macromolecules*, **1997**, *30*, 6398-6400.
28. Matyjaszewski K.; Jo S. M.; Paik H.-j.; Shipp D. A. *Macromolecules*, **1999**, *32*, 6431-6438.
29. Teodorescu M.; Matyjaszewski K. *Macromolecules*, **1999**, *32*, 4826-4831.
30. Senoo M.; Kotani Y.; Kamigaito M. Sawamota M. *Macromolecules*, **1999**, *32*, 8005-8009.
31. Teodorescu M.; Matyjaszewski K. *Macromol. Rapid Commun.*, **2000**, *21*, 190-194.
32. Matyjaszewski K.; Xia J. *Chem. Rev.,* **2001**, *101*, 2921-2990.
33. Matyjaszewski K. *J.M.S.-Pure Appl. Chem.,* **1997**, *A34(10)*, 1785-1801.
34. Matyjaszewski M.; Wang J.-L.; Grimaud T.; Shipp D. A. *Macromolecules*, **1998**, *31*, 1527-1534.
35. Kotani Y.; Kamigaito M.; Sawamoto M. *Macromolecules*, **1999,** *32***,** 2420-2424.
36. Kotani, Y.; Kamigaito M.; Sawamota M. *Macromolecules*, **2000**, *33*, 3543-3549.
37. Ando T.; Kato M.; Kamigaito M.; Sawamoto M. *Macromolecules*, **1996**, *29*, 1070-1072.
38. Simal F.; Demonceau A.; noelsw A. F. *Angew. Chem. Int. Ed*., **1999**, *38*, 538-540.
39. del Rio I.; van Koten G.; Lutz M.; Spek A. L. *Organometallics*, **2000**, *19*, 361-364.
40. Simal, F.; Demonceau A.; Noels A. F. *Tetrahedron Lett.*, **1999**, *40*, 5689-5693.
41. Uegaki H.; Kotani Y.; Kamigaito M.; Sawamoto M. *Macromolecules*, **1997**, *30*, 2249-2253.
42. Uegaki H.; Kotani Y.; Kamigaito M.; Sawamota M. *Macromolecules*, **1998**, *31*, 6756-6761.
43. Brandts J. A. M.; van de Geijn P.; van Faassen E. E.; Boersma J.; van Koten G. *J. Organomet. Chem.*, **1999**, *584(2)*, 246-253.
44. Le Grognec E.; Claverie J.; Poli R. *J. Am. Chem. Soc.*, **2001**, *123*, 9513-9524.
45. Moineau G.; Granel C.; Dubois Ph. Jérôme; Teyssié Ph. *Macromolecules*, **1998**, *312*, 542-544.
46. Lecomte Ph.; Drapier I.; Dubois Ph.; Teyssié Ph.; Jérôme R. *Macromolecules*, **1997**, *30*, 7631-7633.
47. Xia J.; Matyjaszewski K. *Macromolecules*, **1997**, *30*, 7697-7700.
48. Queffelec J.; Gaynor S. G.; Matyjaszewski K. *Macromolecules*, **2000**, *33*, 8629-8639.
49. Matyjaszewski K. *J Phys. Org. Chem.,* **1995**, *8*, 197-207.
50. Greszta D.; Mardare D.; Matyjaszewski K. *Macromolecules*, **1994**, *27*, 638-644.
51. Hawker C. J.; Lee R.; Fréchet J.M. J. *J. Am. Chem. Soc.*, **1991**, *113*, 4583-4588.
52. Turner S. R.; Voit B. I.; Mourey T.H. *Macromolecules*, **1993**, *26*, 4617-4623.
53. Johansson M.; Malmström E.; Hult A. *J. Polym. Sci. Part A Polym. Chem.*, **1993**, *31*, 619-624.
54. Magnusson H.; Malmström, E.; Hult, A. *Macromol. Rapid Commun.*, **1999**, *20*, 453-457.
55. Suzuki M.; Li A, Saegusa I. *Macromolecules*, **1992**, *25*, 7071-7072.
56. Huber T.; Böhme F.; Komber H.; Kronek J.; Luston J.; Voigt D.; Voit B. *Macromol. Chem. Phys.*, **1999**, *200*, 126-133.
57. Kim Y. H. J.; *J. Polm. Sc.i Part A Polym. Chem.*, **1998**, *36*, 1685-1698.

58. Hawker C. J.; Fréchet J. M. J.; Grubbs R. B.; Dao J. *J. Am. Chem. Soc.*, **1995**, *117*, 10763-10764.
59. Gaynor S. G.; Edelman S.; Matyjaszewski K. *Macromolecules*, **1996**, *29*, 1079-1081.
60. Hawker C.J.; Fréchet J.M.J. *J. Chem. Soc.-Perkin Trans 1*, **1992**, *19*, 2459-2469.
61. Wooley K. L.; Fréchet J. M. J.; Hawker C. J. *Polymer,* **1994**, *35*, 4489-4495.
62. Hawker C. J.; Malmström E.; Frank C. W.; Kampf J. P. *J Am Chem Soc.*, **1997**, *119*, 9903-9904.
63. Hovestad N. J.; van Koten G.; Bon S. A. F.; Haddleton D. M. *Macromolecules*, **2000**, *33*, 4048-4052.
64. Leduc M. R.; Hayes W.; Fréchet J. M. J. *J. Polm Sci Part A Polym Chem.,* **1998**, *36*, 1-10.
65. Hedrick J. L.; Trollsås M.; Hawker C. J.; Atthoff B.; Claesson C.; Heise A.; Miller R. D. *Macromolecules*, **1998**, *31*, 8691-8705.
66. Matyjaszewski K.; Miller . PJ.; Pyun J.; Kickelbick G.; Diamanti S. *Macromolecules*, **1999**, *32*, 6526-6535
67. Heise A.; Hedrick J. L.; Trollsås M.; Miller R. D.; Frank C. W. *Macromolecules*, **1999**, *32*, 231-234.
68. Angot S.; Taton D.; Gnanou Y. *Macromolecules*, **2000**, *33*, 5418-5426.
69. Angot S.; Shanmugananda K.; Taton D.; Gnanou Y. *Macromolecules*, **2000**, *33*, 7261-7274.
70. Maier S.; Sunder A.; Frey H.; Mülhaupt R. *Macromol. Rapid Commun.*, **2000**, *21*, 226-230.
71. Heise A.; Diamanti S.; Hedrick J. L.; Frank C. W.; Miller R. D. *Macromolecules*, **2001**, *34*, 3798-3801.
72. Heise A.; Trollsås M.; Magbitang T.; Hedrick J. L.; Frank C. W.; Miller R. D. *Macromolecules*, **2001**, *34*, 2798-2804.
73. Prucker O.; Rühe J. *Langmuir*, **1998**, *14*, 6893-6898.
74. Zhao B.; Brittain W. J. *Prog. Polym. Sci.*, **2000**, *25*, 677-710.
75. Zhao B.; Brittain W.J. *J. Am. Chem. Soc*., **1999**, *121*, 3557-3558.
76. Hussemann M.; Malmström E.; McNamara M.; Mate M.; Mecerreyes D.; Benoit D. G.; Hedrick J. L.; Mansky P.; Huang E.; Russel T. P.; Hawker C. J. *Macromolecules,* **1999**, *32*, 1424-1431.
77. Matyjaszewski K.; Miller P. J.; Shukla N.; Immaraporn B.; Gelman A.; Luokala B.B.; Siclovan T. M.; Kickelbick G.; Vallant T.; Hoffman H.; Pakula T. *Macromolecules,* **1999**, *32*, 8716-8724.
78. Ejaz M.; Yamamoto S.; Ohno K.; Tsuji Y.; Fukuda T. *Macromolecules,* **1998**, *31*, 5934-5926.
79. Kong X., Kawai T.; Abe J.; Iyoda T. *Macromolecules,* **2001**, *34*, 1837-1844.
80. Shah R. R.; Merreceyes D.; Husemann M.; Rees I.; Abbott N. L.; Hawker C. J. Hedrick J. L. *Macromolecules,* **2000**, *33*, 597-605.
81. Kim J.-B.; Bruening M. L.; Baker G. L. *J. Am. Chem. Soc*., **2000**, *122*, 7616-7617.
82. Huang W.; Kim J.-B.; Bruening M. L.; Baker G. L. *Macromolecules*, **2001**, *35*, 1175-1179.
83. von Werne, T.; Patten T. E. *J. Am. Chem. Soc*., **1999**, *121*, 7409-7410.
84. Ejaz M.; Tsuji Y.; Fukuda T. *Polymer,* **2001**, *42*, 6811-6815.
85. Huang X.; Wirth M. J. *Macromolecules*, **1999**, *32*, 1694-169?

86. Guerrini M. M.; Charleux B.; Vairon J.-P. *Macromol. Rapid Commun.*, **2000**, *21*, 669-674.
87. Angot S.; Ayres N.; Bon S. A. F.; Haddleton D. M. *Macromolecules*, **2001**, *34*, 768-774.
88. Kadla J. F.; Gilbert R. D. *Cellulose Chem. Technol.*, **2000**, *34*, 107-216.
89. Ciampolini M.; Nardi N. *Inorg Chem.*, **1966**, *5*, 41-44.
90. Van Krevelen D. W. *"Properties of Polymers"*, **1990**, 3rd edition.

PAPER I

"Atom Transfer Radical Polymerization of Methyl Acrylate from a Multifunctional Initiator at Ambient Temperature",
A.Carlmark, R. Vestberg, E. Malmström,
Polymer, **2002,** *in press*

PAPER II

"Atom Transfer Radical Polymerization from Cellulose Fibers at Ambient Temperature", A. Carlmark, E. Malmström, *J. Am. Chem. Soc.,* **2002**, *124(6)*, 900-901